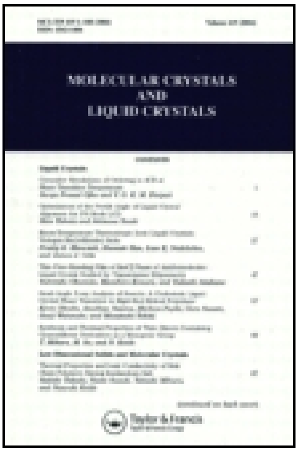

Molecular Crystals and Liquid Crystals Science and Technology. Section A. Molecular Crystals and Liquid Crystals
Publication details, including instructions for authors and subscription information:
http://www.tandfonline.com/loi/gmcl19

Effects of Temperature and Molecular Structure on Rheological Properties of TLCP with Flexible Units in a Main Chain

Soon Kil Kwon [a] & In Jae Chung [a]

[a] Department of Chemical Engineering, Korea Advanced Institute of Science and Technology, Yusong, Taejon, 305-701, Korea

Version of record first published: 24 Sep 2006.

To cite this article: Soon Kil Kwon & In Jae Chung (1994): Effects of Temperature and Molecular Structure on Rheological Properties of TLCP with Flexible Units in a Main Chain, Molecular Crystals and Liquid Crystals Science and Technology. Section A. Molecular Crystals and Liquid Crystals, 254:1, 369-386

To link to this article: http://dx.doi.org/10.1080/10587259408036086

Mol. Cryst. Liq. Cryst. 1994, Vol. 254, pp. 369–386
Reprints available directly from the publisher
Photocopying permitted by license only

Printed in the United States of America

EFFECTS OF TEMPERATURE AND MOLECULAR STRUCTURE ON RHEOLOGICAL PROPERTIES OF TLCP WITH FLEXIBLE UNITS IN A MAIN CHAIN

SOON KIL KWON and IN JAE CHUNG
Department of Chemical Engineering, Korea Advanced Institute of Science and Technology, Yusong, Taejon 305-701, Korea

(Received: February 7, 1994)

ABSTRACT Three kind of thermotropic liquid crystalline (TLC) polyesters with two flexible spacers of decamethylene and hexamethylene in a main chain were synthesized. The homopolymer with decamethylene groups in a main chain (H10) showed two peaks of light intensity in the nematic state during heating and different textures on the temperature in the nematic state. Melting and crystallization transition temperatures by Rheometrics dynamic spectrometer (RDS) and polarized optical microscope (POM) was higher than those by differential scanning calorimetry (DSC). The TLC polyesters showed the dependence of rheological properties on the thermal history at a temperature between the melting temperature measured by DSC and the rheological transition temperature by RDS but above the rheological transition temperature they showed almost the same properties affected negligibly by thermal history. The dependence on thermal history might be caused by both the presence of crystallites in the nematic phase and the effect of supercooling. The existence of crystallites was confirmed by the abrupt decrease of yield stress with temperature. Below the rheological transition temperature spin-drawing was difficult because of fiber breakage and the free-fall fiber showed low orientation, tensile strength, and initial modulus. On the other hand, above it the free-fall fiber had better orientation and higher tensile strength and initial modulus. It was recognized that the rheological transition temperature needed to be defined to determine the temperature for the polymer processing.

INTRODUCTION

Thermotropic liquid crystalline polymers (TLCPs) are generally known to have a high modulus and strength.[1,2] In order to produce excellent TLCPs, it is useful to understand their structures and rheological behaviors.[3,4] Earlier work has shown that the TLCPs display a wide variety of unusual rheological behaviors. These include shear thinning viscosity (pseudoplasticity), yield stress, negative primary normal stress difference, and dependence of flow behavior on thermal and mechanical history.[5-8]

The semiflexible TLCPs have been extensively synthesized and characterized in order to study the structure-property relationships by controlling the position and length of a spacer in a main chain. The effect of flexible spacer on the thermal properties of TLCPs have been well documented in a number of publications.[9-11] Despite of much information on thermal properties, the studies on rheological properties have been limited only to a few semiflexible TLCPs.[3,12,13]

Melting and crystallization temperatures are important for the polymer processing because they affect the mechanical properties of final product. Thus, the melting temperature (rheological transition temperature) needs to be defined under the flow. This study, therefore, focuses on the rheological properties and spinnability of semiflexible TLC polyesters as a function of temperature.

EXPERIMENTAL

Materials

The TLCPs in this work have the following schematic molecular structure:

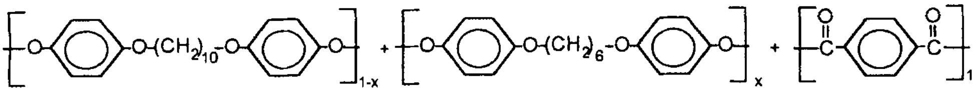

Three samples with codes H10, C50 and H6 are selected and have the X value of 0, 0.5 and 1, respectively. The synthesis method for homopolymers was described by Lenz *et al.*[14,15] and for copolymers by our group.[16,17] Homopolymers and copolymers based on 4,4'-dihydroxy-1,10-diphenoxy decane (DHDPD), 4,4'-dihydroxy-1,6-diphenoxy hexane (DHDPH), and terephthaloyl dichloride (TPC) were prepared by the melt polycondensation at a high temperature and in a high vacuum vessel equipped with stirrer. The DHDPH and DHDPD were synthesized from hydroquinone and α,ω-dibromoalkene following the procedure described by Crater and Cuculo.[18] The characterization of monomers and polymers was described in the previous literatures.[16,17]

Measurements

Differential Scanning Calorimetry and Polarized Optical Microscopy : Differential scanning calorimetry (DSC) measurements were carried out in nitrogen atmosphere with a du Pont Thermal Analyzer 2000. The heating and cooling rates were fixed at 2°C/min. The sample weights were controlled in the range of 9~10 mg. The mesophase textures and the light intensity changes were examined as a function of temperature by using a Leiz polarized optical microscope (POM) equipped with a Mettler GA4 hot stage with heating and cooling rates of 2°C/min.

Rheology : The rheological properties were determined in a nitrogen atmosphere using a Rheometrics Dynamic Spectrometer (RDS 7700) with disc plates of diameter 2.54 cm. The gap between plates and the strain amplitude were fixed at 1.2 mm and 5% at the starting temperature, respectively. Sample discs were prepared by compression molding and dried for 24 hr at 100°C in a vacuum oven in order to remove moisture, prior to the molding and measurements.

Unfortunately, the viscosities of TLCPs were so low that the rheological data at low frequency were scattered because of sensitivity limit of the instrument. Therefore, most data reported here were obtained in oscillatory shear over a frequency range of 1~100 sec^{-1}. However, the TLCPs could be regarded as stable polymers because they showed the good reproducibility in rheological experiment after a number of cycles.

Fiber Spinning

Fiber spinning was carried out by extruding the TLC polyester melt into environmental air at 20°C through a capillary die of an Instron Capillary Rheometer (Model 3211) equipped with a conical die with 90° entry angle, 1.27 mm diameter, and the aspect ratio (*L/D*) of 40. In order to investigate the effect of draw ratio on the molecular orientation, the extrudate of molten state from the die was elongated by take-up apparatus located 60 cm below the capillary rheometer. The mass flow rates was controlled by adjusting the plunger descending speed (*i.e.*, shear rate) and was fixed at a constant shear rate of 125 sec^{-1} while the take-up velocity was varied to change the draw ratio. The draw ratio was determined as the velocity ratio (V_f/V_o) where V_f was the take-up velocity of the fiber and V_o the extrusion velocity at the spinneret. The spinning temperature was also changed as a function of experimental variable.

Measurements of Fiber Properties

X-ray experiments were carried out by using Rigaku X-ray generator with Ni-filtered Cu-K_α radiation in the condition of 30 kV and 40 mA. X-ray diffraction patterns of fibers were taken by using a flat-plate camera with the exposure time of 2 hr. A parallel bundle of fibers were prepared as a specimen for X-ray analysis.

Instron Tensile Tester (Model 4202) was used for tensile tests for fibers with a crosshead speed of 10 mm/min and initial gauge length of 30 mm. All results obtained from tensile tests were based on the average of 10 measurements.

RESULTS AND DISCUSSION

Thermal Properties and Liquid Crystal Textures

Figure 1 shows heating and cooling curves of DSC for three kinds of synthesized TLC polyesters. The heating and cooling rates were fixed at 2°C/min. Two peaks for each of heating and cooling curves were observed. The peak at a lower temperature indicates the transition between crystal and mesophase and that at a higher temperature corresponds to the transition between mesophase and isotropic phase. The exotherm peaks in the cooling process are shown at lower temperatures than the endothermic peaks in the heating process, which indicates the effect of supercooling. The degree of supercooling (*i.e.*, the difference of transition temperatures between heating and cooling curves) of the isotropic-mesomorphic transition is quite small compared to that of mesomorphic-crystal transition.

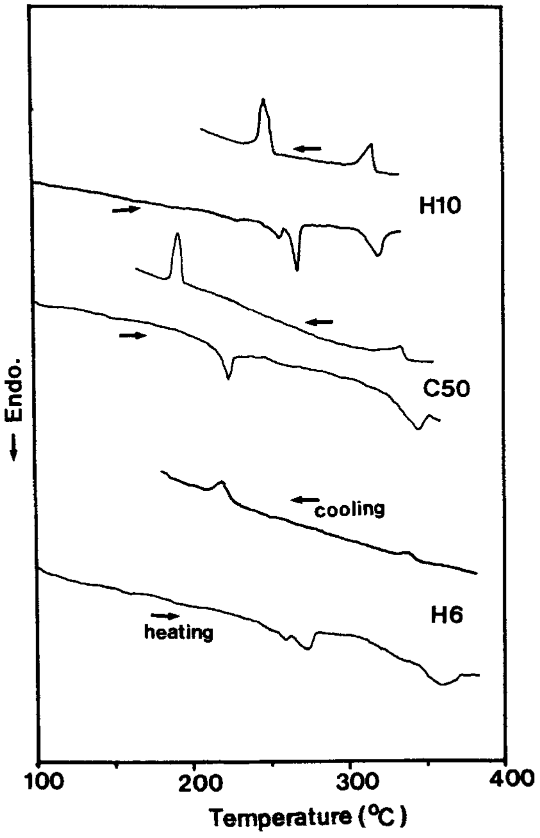

FIGURE 1 DSC curves of synthesized TLCPs in heating and cooling at a rate of 2°C/min.

Depolarizing transmittance was measured to obtain more detailed information about the mesomorphic behavior of the polymers. The transmittance intensity of TLCPs starts to increase from the beginning of melting measured in DSC thermograms, reaches a constant value, and keeps over a broad temperature range above T_m for C50 and H6 samples as shown in Figure 2. The increase of intensity may be caused by the increase of anisotropy within mesophase. However, intensity for H10 decreases rapidly from the temperature 20°C above the melting point and then increased again until it reaches a sharp maximum at about 310°C. This change of intensity is an interesting behavior.

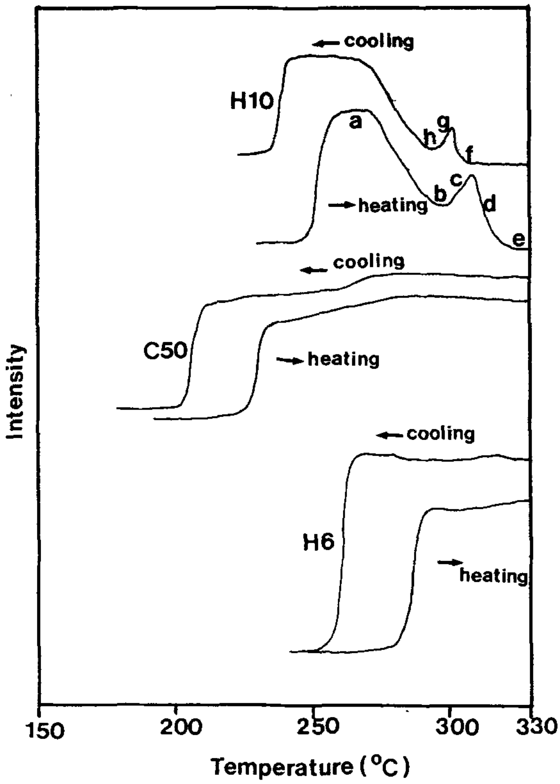

FIGURE 2 Transmittance intensity of TLCPs as a function of temperature in heating and cooling at a rate of 2°C/min.

The mesophase textures of H10 marked with alphabets in Figure 2 are shown in Figure 3. The textures in Figure 3(a) shows the existence of a complex array of dark lines on a light background, which suggests a nematic liquid crystalline phase.[19] When the temperature is increased further, the texture changes to the aggregated domains (Figure 3(b)), which indicates the appearance of isotropic region. The appearance of

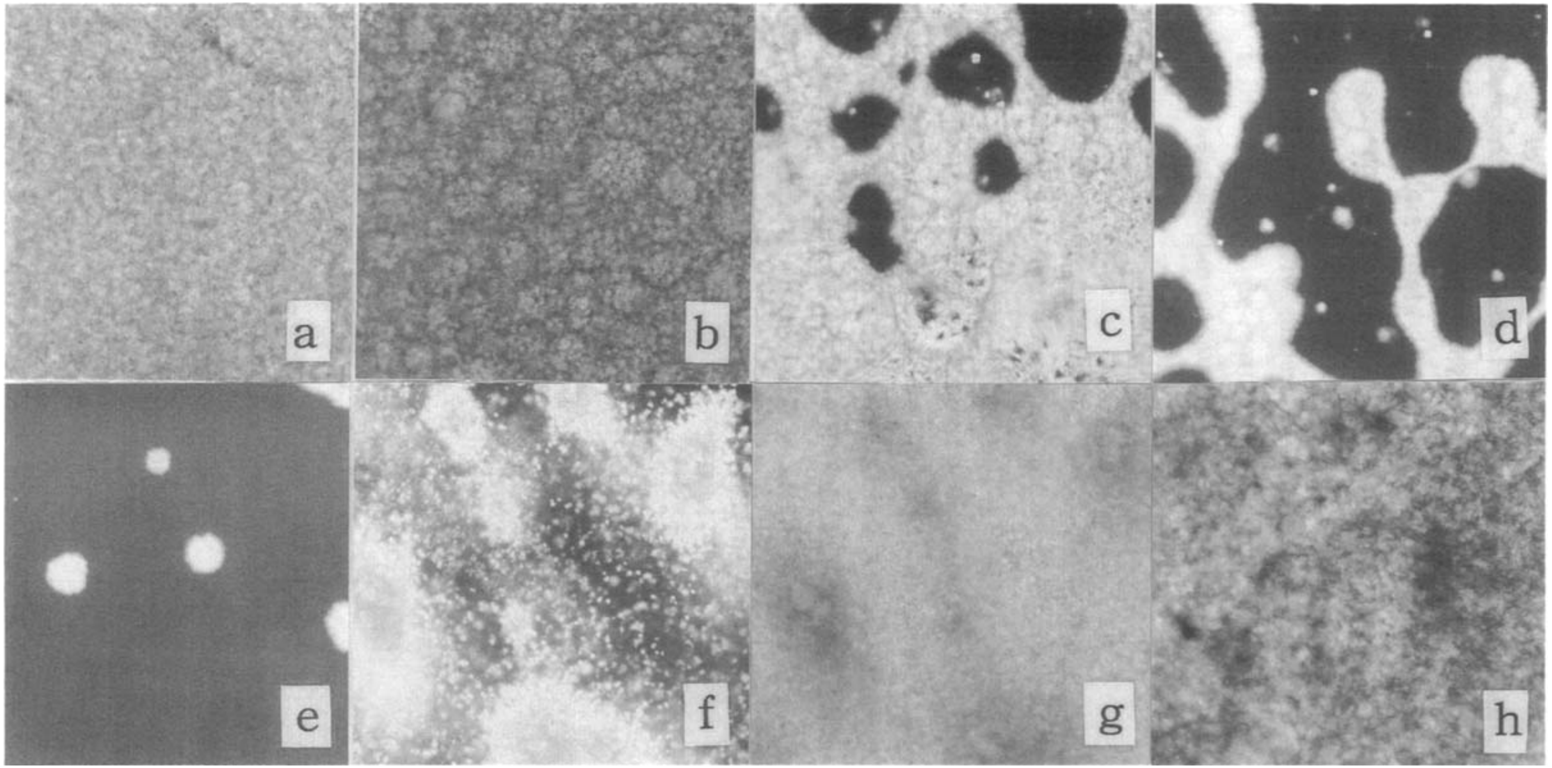

FIGURE 3 **Mesophasic textures of H10 between melting and isotropization temperatures; the alphabets correspond to those in Figure 2.** See Color Plate III.

isotropic region of H10 may be attributed to its long flexible spacer in a main chain because the long flexible spacer often prevent the stability of the liquid crystallinity.[11] Near the isotropic temperature, the dark background indicates an isotropic molten state and has optically anisotropic particles scattered (Figure 3(c)-(e)). Texture changes during the cooling process are given in Figure 3(f)-(h). The textures show reproducibility in heating and cooling processes with the supercooling of phase transition. In addition, the textures of C50 and H6 in the experimental range of temperature show nematic mesophases like Figure 3(a) of H10 even though they are not presented here.

Temperature Dependence of the TLCP Viscoelastic Properties

Figure 4 shows the effects of strain amplitude and deformation history (the number of strain sweeps) on the viscoelastic functions *G′* and *G″* of H10 at 285°C. Nonlinear viscoelastic response begins to appear at 7% strain amplitude. Repetition of the measurement gives rise to a gradual but small decrease in both *G′* and *G″*. C50 and H6 also showed the same patterns and nonlinear response near 7% strain amplitude. Therefore, all measurements were carried out at a fixed strain amplitude of 5% to maintain the linear viscoelasticity.

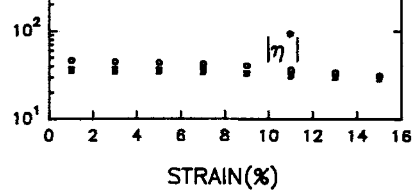

FIGURE 4 Strain amplitude dependence of viscoelastic properties $|\eta^*|$, *G′* and *G″*.

Dynamic data were obtained over heating and cooling sweeps with 10°C intervals at the frequency of 10 sec^{-1}. The samples were loaded on the rheometer at 310°C and held for 1 min. Then the temperature was cooled down to 180°C in the solid state. After keeping for 10 min, heating and subsequently cooling were performed with a rate of 2°C/min. The heating was automatically controlled, whereas the cooling was controlled manually with a very careful attention.

The complex viscosity changes of the TLC polyesters with temperatures are plotted in Figure 5. In the heating mode a dramatic drop in viscosity $|\eta^*|$ is observed at the melting point of each sample. On the other hand, in the cooling mode, a steep increase of the viscosity $|\eta^*|$ is shown near the crystallization temperature. Solidification and rheological melting points are determined by the temperature at which G' and G'' have the same value as suggested by Done and Baird[4] and Masuda *et al.*[5] Masuda *et al.* verified that the transition temperature obtained from the crossover point of G' and G'' was well consistent with that from the apparent activation energy calculating by plotting $\log|\eta^*|$ *versus* $1/T$.

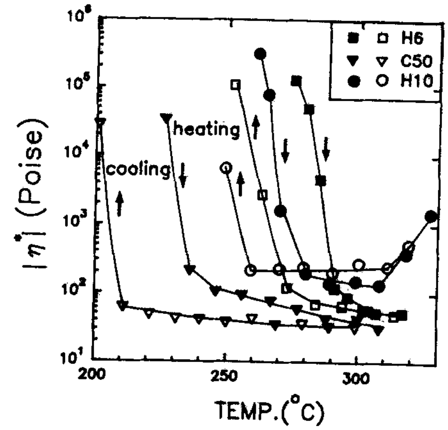

FIGURE 5 Temperature dependence of complex viscosity in heating and cooling at a frequency of 10 sec^{-1}.

Figure 6 shows the temperature dependence of the dynamic moduli (G' and G'') measured with the frequency of 10 sec^{-1}. In the heating mode the storage modulus (G') is larger than the loss modulus (G'') near the melting point. The drop of loss modulus becomes more dominant and larger than storage modulus above the crossover. For H10 the increase of dynamic moduli is observed above 310°C on the heating curve in Figure 6(a), which might imply the gradual transition from nematic phase to isotropic phase.

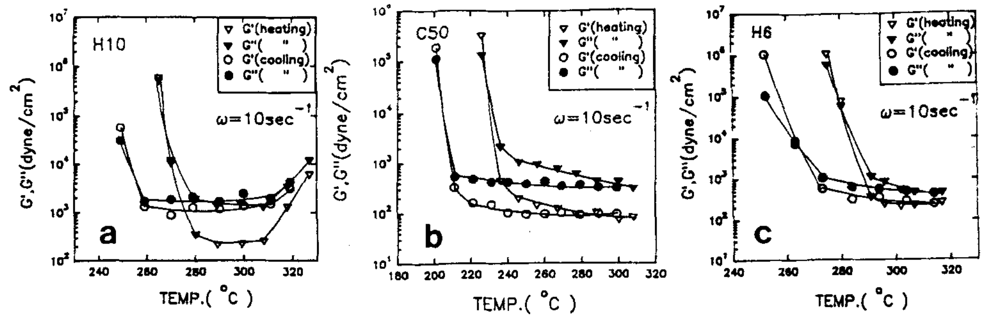

FIGURE 6 Temperature dependence of the dynamic viscoelastic functions G' and G'' in heating and cooling at a frequency of $10\ \text{sec}^{-1}$.

In the cooling process the crossover of the G' and G'' curves is also observed. Generally the crossover temperature shows much lower value in the cooling process than in the heating process, suggesting the effect of supercooling. The temperature difference by supercooling is in the range of 12 to 25°C. The transition temperature measured with the various methods are tabulated in Table I. The transition temperature measured by the POM is the temperature obtained at the inflection point of rapidly changing intensity in Figure 2. In the heating mode the transition temperature measured in dynamic shear flow by RDS is higher than that measured by DSC. The POM results, on the other hand, are consistent with RDS results. For H10, polarized optical microscope shows very different textures between the melting and isotropic temperatures in Figure 3. However, dynamic rheological measurements are insensitive to the change of texture. Only a slight increase of dynamic moduli is encountered at nematic-isotropic transition temperature.

TABLE I Comparison of transition temperatures measured by various methods.

Treatment	Method (condition)	Transition Temperatures (°C)		
		H10	C50	H6
Heating	RDS (about 2°C/min)[a]	268	230	288
	DSC (2°C/min)[b]	254	219	279
	POM (2°C/min)[c]	266	233	284
Cooling	RDS (about 2°C/min)	256	207	263
	DSC (2°C/min)	236	193	243
	POM (2°C/min)	255	208	262

[a] Crossover point obtained from the G' and G'' curves in Figure 6.

[b] Maximum peak point obtained from the thermograms in Figure 1.

[c] Inflection point obtained from the intensity curves in Figure 2.

Effect of Thermal History on Viscoelastic Properties

The effect of thermal history on viscoelastic properties was investigated above and below the rheological transition temperature in the heating mode. Frequency dependence of the viscoelastic functions G', G'', and $|\eta^*|$ of TLC polyester was measured under the controlled thermal history. The sample was kept at 310°C for 1 min, cooled down to the test temperature, kept for 10 min and tested for the first run. The sample was further cooled down to 180°C and kept for 10 min. It was heated to the test temperature, kept for 10 min and tested for the second run. After the sample was further heated to 310°C and kept for 10 min, it was cooled down to the test temperature, kept for 10 min and tested for the third run.

G', G'', and $|\eta^*|$ at a high temperature above the rheological transition temperature are little affected by the thermal history and have almost a constant value independent of frequency (Figure 7(a)-(c)). This suggest that the thermodynamic equilibrium is attained at that temperature.

In contrast with the above results, thermal history at a low temperature below the transition temperature affects significantly the rheological properties. As shown in Figure 7(d)-(f), viscoelastic properties obtained in the second test show much higher values than those obtained in the first test when the test temperature is between melting temperatures measured by DSC and RDS. The third test shows almost the same viscoelastic properties as the first test, displaying a low viscoelastic properties. This thermoreversibility suggests that the modulus growth in the second test results from a physical change rather than a chemical change. The increase of viscoelastic properties in the second test is thought perhaps to be related to the presence of residual crystal.

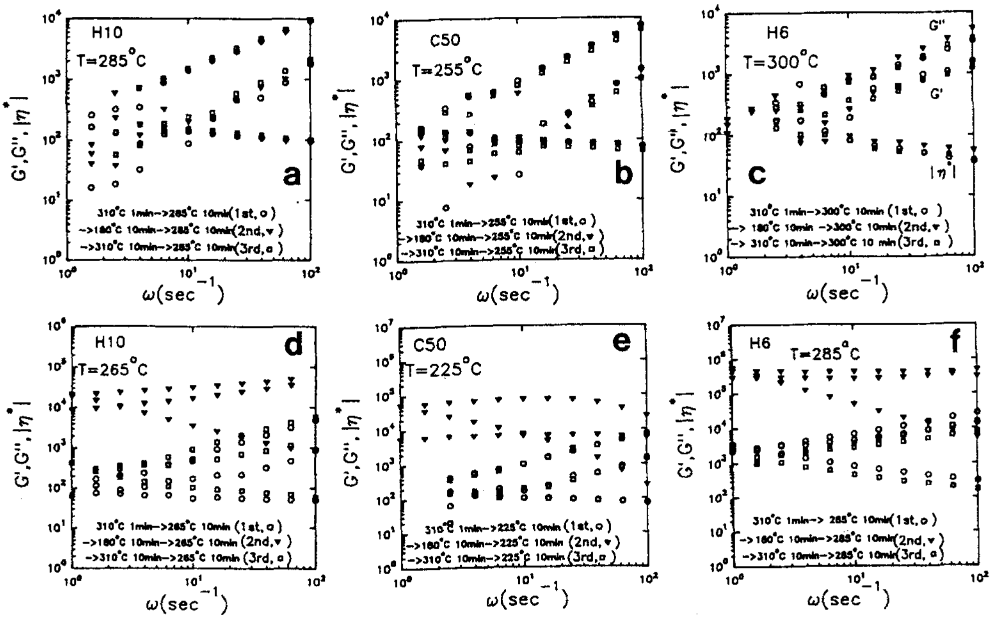

FIGURE 7 Frequency dependence of the viscoelastic functions $|\eta^*|$, G' and G'' under the controlled thermal history.

It has been known that yield stress is observed when liquid crystal and solid crystallites coexist.[7] If the temperature is not high enough to melt all the crystallites, a large yield stress is required to initiate the flow. Yield stresses for the three samples are obtained by extrapolating the shear stress ($|\eta^*| \times \omega$) to the zero frequency as shown in Figure 8(a). The estimated yield stresses are plotted as a function of temperature in Figure 8(b). Below the rheological transition temperature, the yield stresses are unusually high, indicating that the samples are not completely melted.

The yield stress abruptly decreases as the temperature approaches the rheological transition temperature but it does not disappear even if the temperature increases further. It has been known that textured liquid crystalline polymers have a *piled polydomain structure* and reveal the yield stress.[21] Therefore, the presence of the yield stress for our TLC polyesters at higher temperature than the transition temperature are believed to be related to the *piled polydomain structure*.

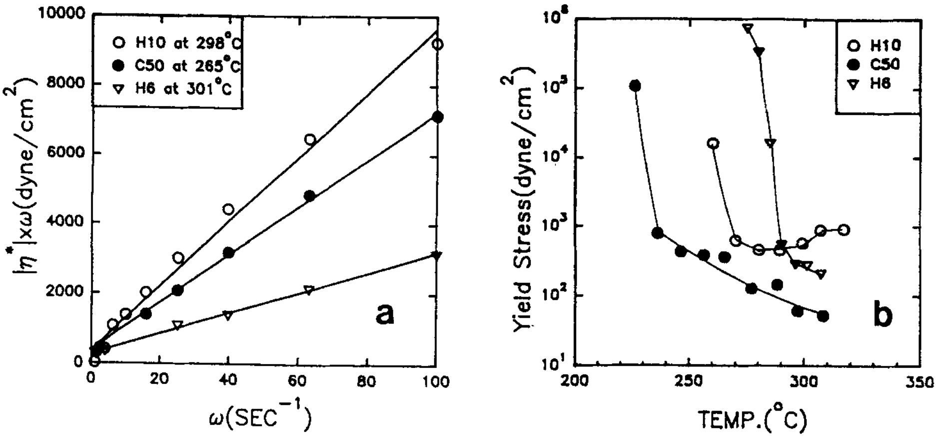

FIGURE 8 (a) Extrapolation of the shear stress to the zero frequency. (b) The yield stress plotted as a function of temperature.

In conclusion, below the rheological transition temperature the viscoelastic properties of the TLC polyesters are affected strongly by the thermal history but above the transition temperature they show almost the same values negligibly affected by the thermal history. The PHB60/PET40 material showed the dependence of viscoelasticity on thermal history in the wide range of temperature above the melting point of PET unit because of the coexistence of two phases, the solid state of PHB unit and liquid region of PET unit.[5] On the other hand, the temperature range in our TLC polyesters is narrow, that is, shown in smaller range of 9~14°C above melting point and is not originated from the phase separation but from the unmelted crystal.

Effect of Extrusion Temperatures on the Orientation and Mechanical Properties of the Spun Fibers

The X-ray diffraction diagrams for the TLC polyesters extruded through a capillary die below and above the rheological transition temperature are shown in Figure 9. The free-fall extrudates produced below the transition temperature are poorly oriented due to the presence of unmelted crystallites. Above the transition temperature they have a high orientation, which indicates that all the liquid-crystalline domains are deformable during the flow, and all individual molecular chains have sufficient thermal mobility to be aligned in the flow direction.

TABLE II Tensile properties of the TLCPs extrudated below and above rheological transition temperatures

Sample Codes	Tensile Strength (MPa)[a]		Tensile Modulus (GPa)[b]		Elongation (%)	
	Below	Above	Below	Above	Below	Above
H10	37.85	64.05	0.94	1.49	8.62	11.21
C50	46.80	124.89	0.83	2.18	5.26	8.16
H6	190.90	225.96	5.12	5.39	4.41	4.53

[a] Ultimate break strength
[b] Initial modulus

The tensile properties of TLC polyesters are tabulated in Table II. The extrudates above the transition temperature have higher tensile strength and initial modulus than those below the transition temperature. Spin-drawing was difficult below the transition temperature because of fiber breakage. On the other hand, the spinnability above the transition temperature was good and the orientation was improved with increasing the draw ratio. The X-ray diffraction diagrams of H10 fiber shows a higher orientation as the draw ratio increases in Figure 10. The azimuthal breadth in the strongest equatorial reflection decreases with draw ratio, which indicates better fiber orientation. To determine the qualitative indication of orientation, the orientation angle is obtained from the X-ray diffraction diagram.[20] The angle of the wide-angle arc, as shown schematically inside of Figure 11, indicates the degree of orientation: a

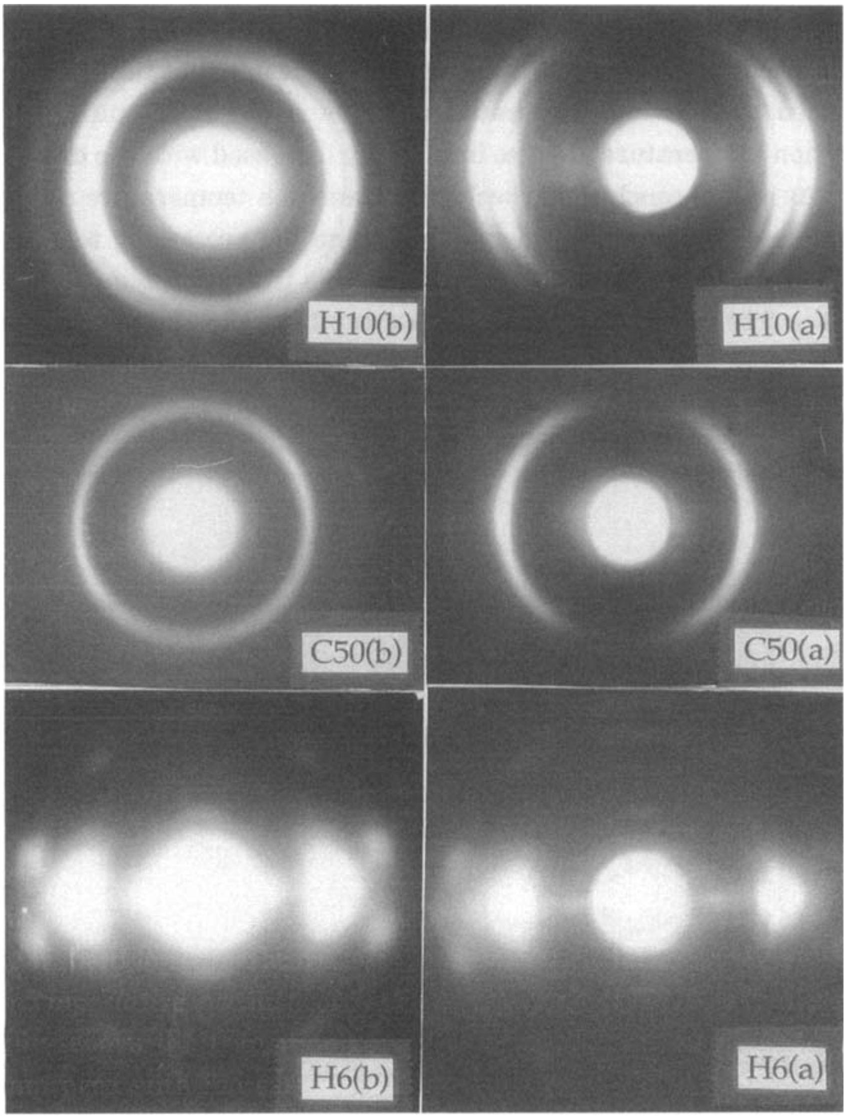

FIGURE 9 The X-ray diffraction diagram of TLC polyesters extruded below (b) and above (a) the rheological transition temperature.

small angle of represents the high orientation of a fiber. In Figure 11 the orientation angles and modulus are plotted against the draw ratio. The open symbols are the orientation angle of fiber spun at a fixed draw ratio, and the filled symbols correspond to values of modulus. Generally the values are decreased with draw ratio. This indicates that the orientation is enhanced by drawing. The initial modulus of the fiber spun above the transition temperature are also intensively increased with the draw ratio.

As a final conclusion, rheological transition temperature needs to be defined and measured in order to determine the processing temperature. The fiber could not be spun easily below this transition temperature and even the free-fall extrudates through a capillary die showed poor tensile properties.

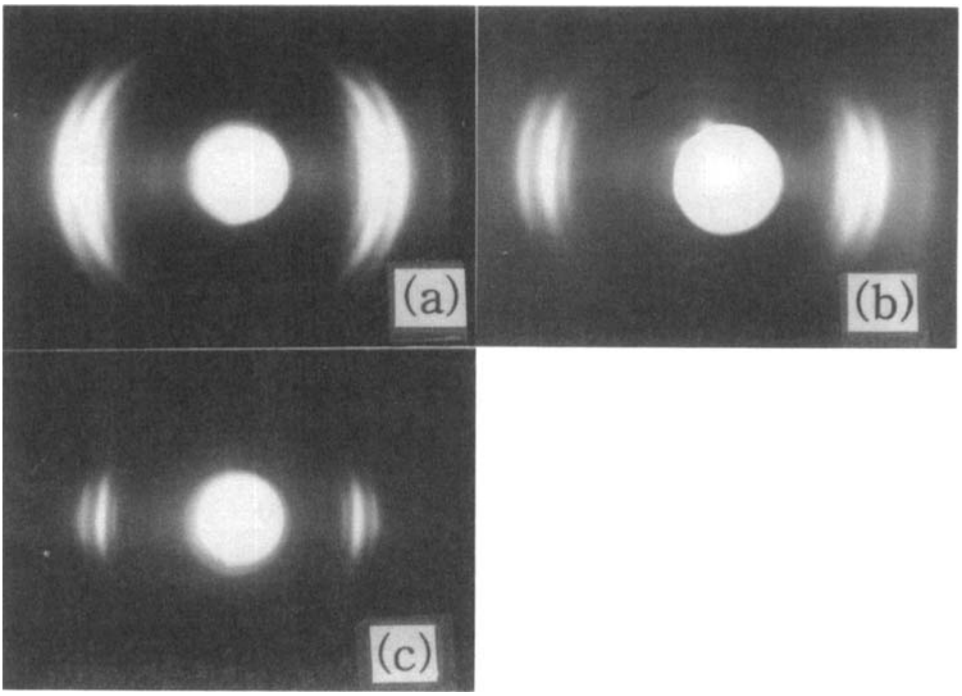

FIGURE 10 The X-ray diffraction diagrams of fiber H10 with draw ratio: (a) draw ratio=1.0, (b) 10.4, and (c) 17.4.

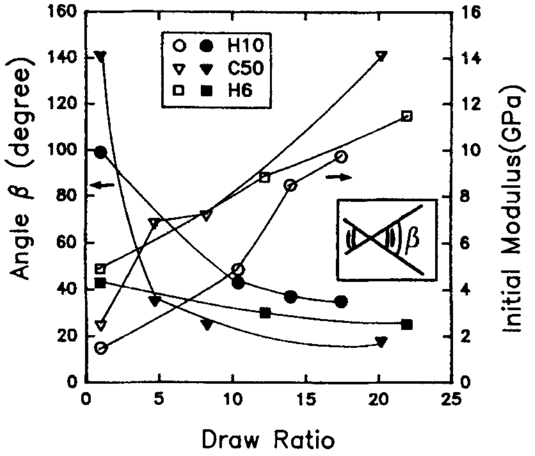

FIGURE 11 The orientation angle and initial modulus of as-spun fibers plotted as a function of draw ratio.

REFERENCES

1. E.B. Priestley, P.J. Wojtowicz, and P. Sheng, *Introduction to Liquid Crystals* (Plenum Press, N.Y., 1979).
2. A. Ciferri (ed.), *Liquid Crystallinity in Polymers* (VCH Publishers, N.Y., 1991).
3. D.S. Kalika, M.R. Shen, X.M. Yu, and M.M. Denn, *Macromolecules*, **23**, 5192 (1990).
4. D. Done and D.G. Baird, *Polym. Eng. Sci.*, **30**, 989 (1990).
5. T. Masuda, K. Fujiwara, and M. Takahashi, *Intern. Polym. Processing*, *6*, 225 (1991).
6. S.M. Guskey and H.H. Winter, *J. Rheol.*, **35**, 1191 (1991).
7. D.-K. Yang and W.R. Krigbaum, *J. Polym. Sci., Polym. Phys. Ed.*, **27**, 1837 (1989).
8. K.F. Wissbrun, *Brit. Polym. J.*, 163 (Dec. 1980).
9. A. Abe, *Macromolecules*, **17**, 2280 (1984).
10. V. Arrighi, J.S. Higgins, R.A. Weiss, and A.L. Cimecioglu, *Macromolecules*, **25**, 529 (1992).

11. C.K. Ober, J.-I. Jin, and R.W. Lenz, *Adv. Polym. Sci.*, **59**, 103 (1984).
12. S.K. Bhattarcharya and A. Misra, *Polym. Eng. Sci.*, **30**, 124 (1990).
13. K.F. Wissbrun, *J. Polym. Sci., Polym. Phys. Ed.*, **20**, 1835 (1982).
14. G. Chen and R.W. Lenz, *J. Polym. Sci., Polym. Chem. Ed.*, **22**, 3189 (1984).
15. S. Antoun, R.W. Lenz, and J.-I. Jin, *J. Polym. Sci., Polym. Chem. Ed.*, **19**, 1901 (1981).
16. B.Y. Shin and I.J. Chung, *Polym. J.*, **21**, 851 (1989).
17. Y.S. Kim and I.J. Chung, *Polym. J.*, **23**, 1339 (1991).
18. D.H. Crater and J.A. Cuculo, *J. Polym. Sci., Polym. Phys. Ed.*, **21**, 2219 (1983).
19. D. Demus and L. Richer, *Textures of Liquid Crystals* (Verlag Chemie, Weinheim, 1978).
20. H. Muramatsu and W.R. Krigbaum, *J. Polym. Sci., Polym. Phys. Ed.*, **25**, 803 (1987).
21. T. Asada, H. Muramatsu, R. Watanabe, and S. Onogi, *Macromolecules*, **13**, 867 (1980).